Proceedings of ASME Turbo Expo 2003
Power for Land, Sea, and Air
June 16–19, 2003, Atlanta, Georgia, USA

GT2003-38251

Predictions of Cooling From Dirt Purge Holes Along the Tip of a Turbine Blade

E. M. Hohlfeld, J. R. Christophel, E. L. Couch, K. A. Thole
Mechanical Engineering Department
Virginia Polytechnic Institute and State University
Blacksburg, VA 24060

ABSTRACT

The clearance gap between the tip of a turbine blade and its associated shroud provides a flow path for leakage from the pressure side of the blade to the suction side. The tip region is one area that experiences high heat transfer and, as such, can be the determining factor for blade life. One method for reducing blade tip heat transfer is to use cooler fluid from the compressor, that exits from relatively large dirt purge holes placed in the tip, for cooling purposes. Dirt purge holes are typically manufactured in the blade tip to extract dirt from the coolant flow through centrifugal forces such that these dirt particles do not block smaller diameter film-cooling holes. This paper discusses the results of numerous computational simulations of cooling injection from dirt purge holes along the tip of a turbine blade. Some comparisons are also made to experimental results in which a properly scaled-up blade geometry (12X) was used to form a two-passage linear cascade. Computational results indicate that the cooling achieved through the dirt purge injection from the blade tip is dependent on the gap size as well as the blowing ratio. For a small tip gap (0.54% of the span) the flow exiting the dirt purge holes act as a blockage for the leakage flow across the gap. As the blowing ratio is increased for a large tip gap (1.63% of the span), the tip cooling increases only slightly while the cooling to the shroud increases significantly.

INTRODUCTION

Turbine blades are exposed to extremely harsh operating conditions that greatly affect the overall life and performance of a gas turbine engine. The tip region of a turbine blade is one area that experiences cycle accumulation damage from oxidation, burning, and stresses from both thermal and mechanical forces. To maintain a clearance between the blade tip and outer shroud, there is a tolerance gap that is specified in most turbine designs. This gap distance can change during the course of a flight as a result of a range of operating conditions for the turbine. Unfortunately, this gap provides a path for flow leakage across the blade tip. The tip gap flow is driven by a pressure differential from the pressure side to the suction side of the blade, but is limited by the viscous forces as the fluid comes into contact with the walls of the gap. This leakage flow is typically hot gas that has migrated up the pressure side of the blade. In a typical engine the extremely high temperatures coupled with the highly turbulent flow in the tip region cause heat transfer to be unusually high in a region that is difficult to cool.

This study investigates the benefits of using a recessed cavity within the tip fed by coolant air from two dirt purge holes. To some extent the dirt purge cavity resembles the geometry seen in a squealer tip, but this cavity does not extend over the entire tip region. Instead, it extends only over a small area in the front portion of the blade. The dirt purge has two primary functions that include the following: it allows for dirt ingested by the compressor to be exhausted into the turbine without clogging film cooling holes, and it provides coolant to the front portion of the blade tip. Centrifugal forces help to insure that the debris is exhausted through the dirt purge holes that are relatively large compared to film cooling holes. The dirt purge cavity is present to insure that during blade rubbing the purge holes remain open.

A detailed computational study of a turbine blade with a dirt purge cavity was performed to examine both flow and cooling characteristics when exposed to two tip gap sizes and various blowing ratios. Computational results will be discussed and compared when possible to experimental measurements. In particular, the focus will be on the effects of various tip gaps and blowing ratios on adiabatic effectiveness levels along the blade tip and along the shroud.

PAST STUDIES

Over the past 50 years there have been numerous studies that have addressed tip leakage effects with the primary emphasis being to decrease the leakage flow in order to reduce losses in turbine efficiencies. The leakage that occurs across the tip gap from the pressure to suction sides is inherent to the blade and is a function of the blade loading. A second dictating factor on the tip leakage is the gap distance between the blade tip and shroud. Because this gap is relatively small, viscous effects in the gap are important. One important flow feature that has been identified by past investigations includes a tip leakage vortex, which results from a velocity differential between the

main gas path flow and the tip leakage flow as it exits from the suction side of the gap. Another important flow feature, which has not only been identified by computational fluid dynamics (CFD) studies but also heat transfer studies, is the presence of a flow separation zone along the pressure side of the blade tip as the passage flow enters the gap. The blade tip is typically modeled to have a relatively sharp corner thereby lending the flow to be separated in this area.

As of late, tip heat transfer studies have become of primary interest whereby a comprehensive summary has been discussed by Bunker [1]. Several distinct regions have been identified by a number of recent investigators (Bunker et al [2], Papa et al [3], and Azad et al [4]) through measured heat transfer coefficients along the blade tip region. One region, located in the thickest part of the blade, has been shown to have low convective heat transfer coefficients as a result of low convective velocities. In contrast, two regions having the highest heat transfer coefficients are the leading edge region and along the pressure side of the blade where the flow separation region is present. The general consensus among these papers is that with a larger tip gap, overall heat transfer coefficients increase due to the larger leakage flows. Acharya, et al [5] reported computational studies using the same code and methods reported in our paper to directly compare with the data given by Azad et al [4]. Reasonable agreement was found between the experiments and computations.

One method for reducing the leakage flow while also improving the thermal environment for the blade tip is to inject coolant in the tip region. Not many studies are available in the open literature documenting film-cooling from a tip. Kim, et al [6] presents a summary of the experimental work that Dr. D. Metzger performed in this area. Several key findings from his work include the following: there is only a weak effect of the relative motion between the blade and shroud and there is a strong dependency of tip film-cooling on hole shapes and injection locations. Kwak and Han [7] reported experimental results for tip blowing with a range of tip gap sizes and range of blowing conditions. Cooling holes were placed along the pressure surface at a 30˚ breakout angle and on the tip surface at a 90˚ angle. Their results indicated an increase in film effectiveness and heat transfer coefficients with increased tip gap sizes. Higher blowing ratios increased the film effectiveness on the tip while decreasing the heat transfer coefficients. In particular, the cooling holes along the pressure side acted as a flow resistance for the tip leakage flow resulting in lower heat transfer coefficients.

Another method that is commonly used for reducing leakage flow in the tip gap is to use a squealer-tip, which acts as a seal by increasing the flow resistance. Experimental work using a two-dimensional channel with a grooved tip with blowing was studied by Metzger et al [8] and Chyu et al [9]. They found the results to be highly dependent on the coolant injection.

In summary, there are only a handful of studies that have addressed blowing in the tip gap region. While squealer tips are somewhat relevant to the work presented in our paper, the size of the dirt purge cavity is smaller in extent, but similar in depth, to that of typical squealer tip design. Moreover, none of these past studies have addressed a realistic aero-engine design that contains the presence of the dirt purge geometry with blowing. For that reason, the work we are presenting in this paper is unique to the literature in the field.

TIP GAP GEOMETRY AND TEST CASES

The blade geometry used for this work represents a modified design for the first stage of a gas turbine. The modifications from the original engine geometry were made to insure correctly scaled driving pressures across the tip gap when operating in a low-speed testing environment. To ensure good measurement resolution while matching engine Reynolds numbers and flow angles in low-speed wind tunnel tests, a 12X scaled turbine blade was designed. The turbine blade geometry is two-dimensional having no variation in the span direction. A summary of geometry and flow conditions are given in Table 1.

The dirt purge geometry found within the blade tip is shown in Figure 1. Two different tip gap heights were considered at 0.54% and 1.63% of the full blade span. One of the first studies completed was a flat tip with no dirt purge cavity. This case allowed for comparisons to be made to experimental measurements. While the focus of our current paper is not on the experimental results, there are a few comparisons between predictions and experiments. The experiments, which will be the subject of a future paper, included simulations of a 12X blade model in a low speed wind tunnel facility. The test section consisted of a two passage, linear cascade in which the flow angles were matched by properly staggering the blades. Through the use of tailboards and sidewall bleeds, periodicity between the two passages was achieved. Good agreement was indicated between the non-dimensional pressure distribution at the mid-span obtained from computational and experimental measurements as shown in Figure 2.

Table 1. Geometry and Flow Conditions

Parameter	Value
Scaling Factor	12X
axial chord/true chord	0.66
pitch/true chord	0.81
span/true chord	1.03
Re_{in}	$2.1x10^5$
Inlet Angle	16.5°
Coolant to Freestream ΔT	20°C

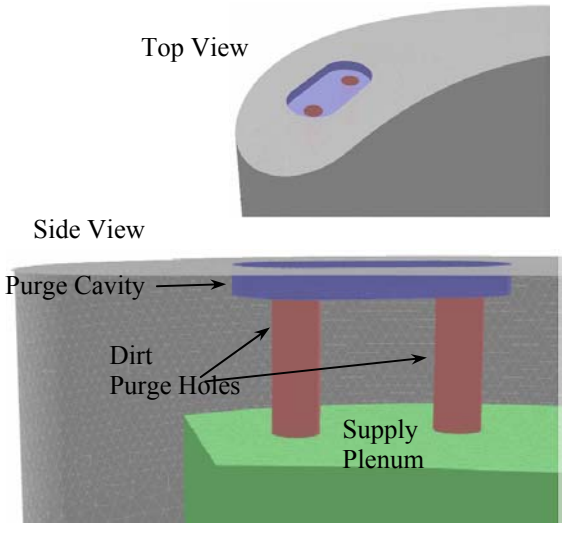

Figure 1. Illustration of the blade and dirt purge geometry.

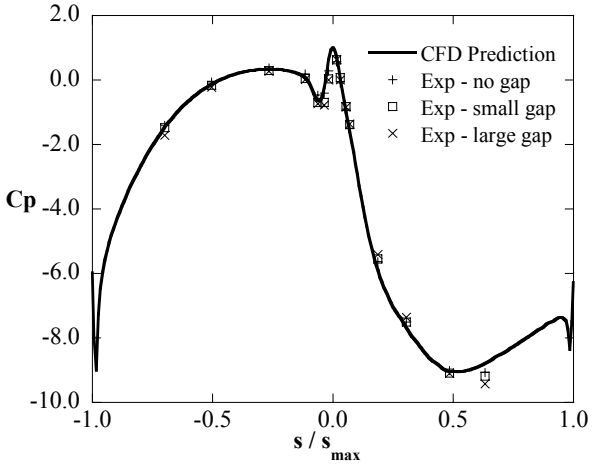

Figure 2. CFD prediction and measured pressure distribution at the vane mid-span location.

COMPUTATIONAL METHODOLOGY

A commercially available computational fluid dynamics (CFD) code, Fluent 6.0 [10] was used to perform all simulations. Fluent is a pressure-based, incompressible flow solver that can be used with structured or unstructured grids. An unstructured grid was used for the study presented in this paper. Solutions were obtained by numerically solving the Navier-Stokes and energy equation through a control volume technique. All geometric construction and meshing were performed with GAMBIT.

Computations were performed on a single turbine blade exposed to periodic conditions along all boundaries in the pitch direction. Inlet conditions to the model were set as a uniform inlet velocity at approximately one chord upstream of the blade. Because the injected flow from the tip gap was at most 0.38% of the passage flow, the inlet flow was maintained as the same for all simulations. Flow angles were set to match those conditions of the experiments as well as the scaled values for the engine while the turbulence levels and mixing length were set to 1% and 0.1 m, respectively. A plenum within the blade cavity provided coolant flow to the dirt purge holes at a temperature difference of 20°C below that of the core flow (matching that simulated in the experiments). The density ratio of the coolant to the mainstream was nearly one (~1.06) for all of the cases simulated. The amount of coolant was specified as a mass flowrate boundary condition entering the plenum for the dirt purge. Flow entered the tip region through the two cylindrical dirt purge holes. An outflow boundary condition was applied at 1.5 chords downstream of the blade. Only the half of the flow passage was modeled. Comparisons were made between the predicted results for the entire blade span as compared with that for only 50% of the span. No differences were noted in the full and half span models. As such, only half the span was simulated extending from the blade mid-span to the blade shroud. The boundary condition at the mid-span of the domain was set as a slip wall (frictionless) while a no-slip boundary condition was applied at the tip, shroud and all other surfaces.

To ensure a high quality mesh, the flow passage was divided into multiple volumes, which allowed for more control during meshing. The tip gap region was of primary concern and was composed entirely of hexahedral cells with an aspect ratio smaller than three. Below the tip gap region within the blade were four additional volumes that included the dirt purge cavity, the two dirt purge holes, and the plenum. The dirt purge cavity and holes were meshed in a manner similar to the tip gap, using a fine hexahedral element. The plenum was meshed with coarser tetrahedral elements. The main flow passage was generally meshed with a coarse tetrahedral mesh with the following two exceptions: the faces around the blade were composed of tetrahedral cells, and a separate volume around the tip gap extending down the blade from the tip gap to approximately 15% of the span. This separate volume, meshed with tetrahedral cells around the tip region, served as a transitional zone between the extremely tight tip gap mesh and the coarser passage mesh.

All computations were performed using the RNG k-ε turbulence model with non-equilibrium wall functions whereby the near-wall region was resolved to y^+ values ranging between 30 and 60. An extremely useful feature of Fluent involves the ability to adapt the grid based on flow solutions. This can be used for obtaining grid-independent results. Mesh insensitivity was confirmed through several grid adaptions based on viscous wall values, velocity gradients, and temperature gradients. Typical mesh sizes were composed of 1.8 million cells with 50% of the cells in and around the tip gap region. After adapting from a mesh of 1.7×10^6 to 2.2×10^6, the pitchwise-averaged effectiveness predictions on the tip were found to vary by only $\Delta \overline{\eta} = \pm 0.007$ at a level of $\overline{\eta} = 0.40$.

The convergence of residuals for continuity, *x*-momentum, *y*-momentum, *z*-momentum, *k* and ε were resolved to levels of 10^{-4} for all entities with the exception of the energy equation which was set to a level of 10^{-7}. Typical computations required 1200 iterations for convergence to be met.

EFFECT OF TIP HEIGHT, GEOMETRY, AND BLOWING

A set of simulations focused on investigating the effect of tip gap geometry, tip gap height, and tip gap blowing as indicated in Table 2. With regards to the tip gap height, two different gaps relative to the span were investigated including gaps that were 0.54% (small tip gap) and 1.63% (large tip gap). Through the remainder of this paper these two tip gaps will be referred to as small and large tip gaps. With regards to the tip geometry, two cases were investigated that included the following: i) a flat tip with no purge cavity and ii) a tip with a purge cavity, with coolant injecting from the dirt purge holes. The simulation of the cavity with no blowing is relevant from a practical standpoint modeling a case where the purge holes are blocked. Lastly, with regards to the blowing from the dirt purge holes, two blowing ratio cases at each tip gap height were computed with a coolant flowrate that was 0.19% and 0.29% of the primary core flow. These flowrates were chosen based on realistic engine conditions. For the large tip gap a number of blowing ratios were simulated.

Table 2. Experimental and Computational Test Matrix.

Tip Gap (% Span)	Coolant Flow (% Passage Flow)	CFD	Exp.
Small (0.54)	Flat tip	X	X
	0, purge cavity	X	
	0.19, 0.29	X	
Large (1.63)	Flat tip	X	X
	0, purge cavity	X	
	0.05, 0.10, 0.19, 0.29, 0.38	X	

Effect of Tip Gap Height

Figures 3a-d show measured and predicted static pressure distributions along the shroud for two different tip gap heights. Figure 4a-b show the flow fields and static pressure contours in the tip gap region with the plane taken normal to the pressure side of the blade at the entrance to the gap (shown as a black line in Figure 3a and c). Note that the same vector scales are maintained for these two flow field comparisons. For the experimental measurements, a total of 122 static pressure taps were installed along the shroud with the location of these taps determined using the pre-test CFD predictions of the static pressure distribution. The white dots in Figure 3d show the pressure tap locations for the experiments on the shroud. Note that the one difference between the computations and experiments is that for the experiments a turbulence level at the inlet to the blade is 12% whereas the computations were completed for only 1% freestream turbulence.

Comparisons between the measured and computed static pressure distributions for the smaller tip gap indicate relatively good agreement in terms of the overall level as well as the contour locations. For the large tip gap, shown in Figure 3c-d, lower static pressure contours occur relative to the small tip gap, shown in Figure 3a-b, indicating more leakage across the tip. While the measured pressure contours indicate a slightly larger flow across the gap than the predictions, the overall trends between the measured and computed static pressure contours agree fairly well. It is clear for the larger tip gap that there is a lower pressure on the shroud near the mid-chord along the pressure side of the blade. This low pressure region is a result of the vena-contracta effect as the leakage flow enters into the tip gap as shown in Figure 4b. Figure 4a shows that the small tip gap has a smaller lower pressure region and lower gap velocities than the large tip gap.

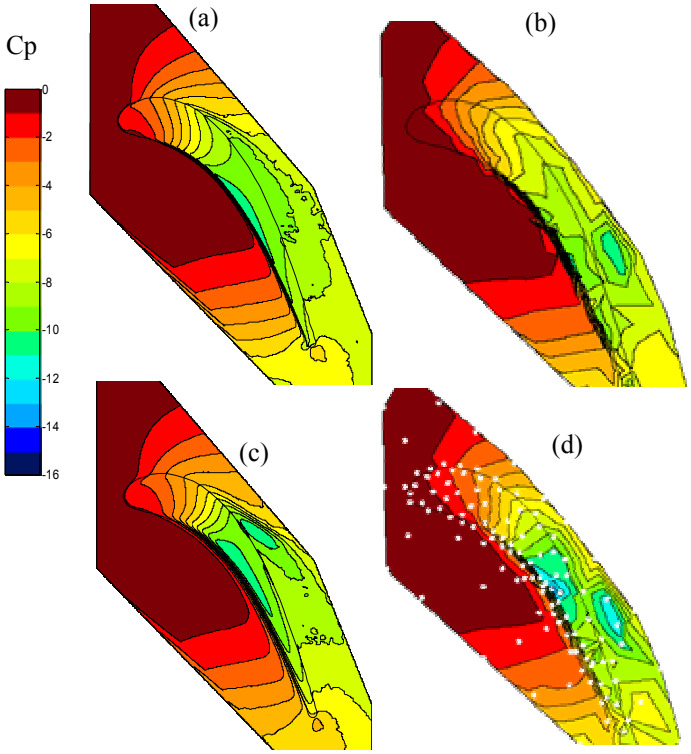

Figures 3a-d. Static pressure contours on the shroud as a) predicted and b) measured for the small tip gap, and as c) predicted and d) measured for the large tip gap.

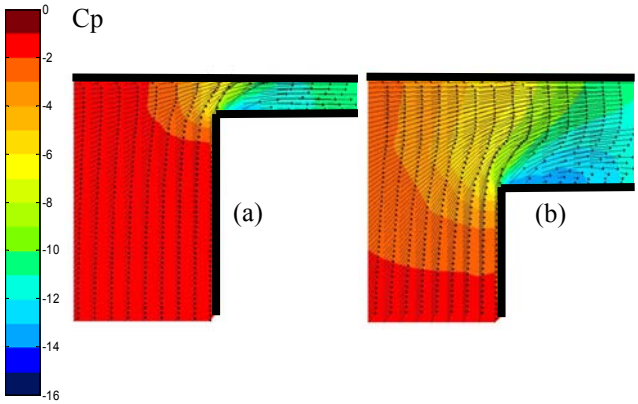

Figures 4a-b. Static pressure contours and velocity vectors in a plane cut through the tip gap in the mid-chord region as depicted in Figure 3a and c for a) a small tip gap and b) a large tip gap.

Figures 5a-d present results for the small and large tip gaps with a flat blade tip and a dirt purge cavity with no blowing. Figures 5a and 5b provide the streamline patterns where these streamlines are colored by the spanwise velocity component. Note that the positive direction for the spanwise component is towards the shroud. These streamlines were released from the same height relative to the tip gap at 1.5 times the tip gap height below the shroud. The actual release height was further from the shroud for the large tip gap, but the same relative to the gap size. It is clear that the fluid located this distance from the shroud is being convected across the tip. The CFD simulations have indicated that the tip gap fluid originates from the pressure side of the airfoil as far away as 20 (small) gap heights below the shroud. The gap flow is being swept toward

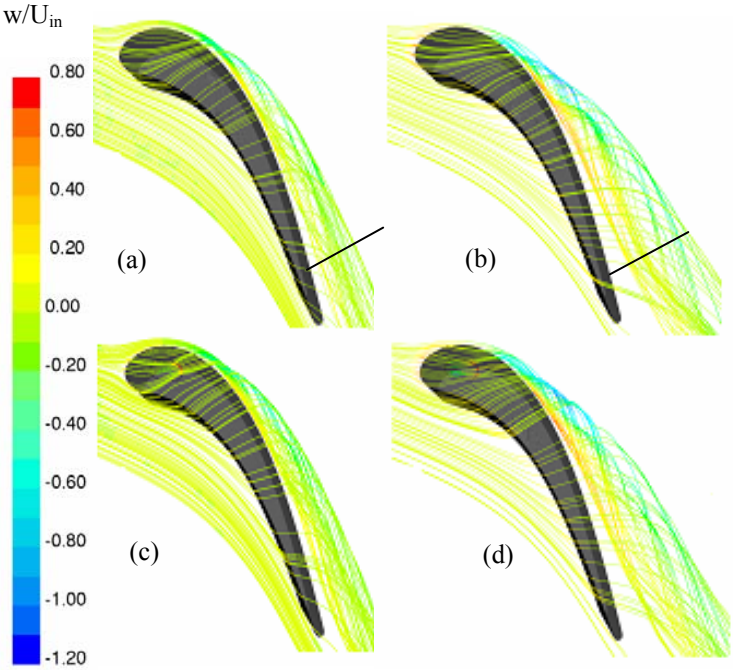

Figures 5a-d. Streamlines released from 1.5 tip gap heights below the shroud colored by the spanwise velocity for a) small tip gap with a flat blade tip, b) large tip gap with flat blade tip, c) small tip gap with a non-flowing cavity, and d) large tip gap with a non-flowing cavity.

the shroud along the pressure side of the airfoil prior to entering the tip gap. For the large gap, the leakage fluid was traced to a location that was 11 (large) gap heights below the shroud.

As can be seen from the streamlines in Figure 5a and 5b, the dominant effect of the tip gap size is on the formation of the leakage vortex, which is much larger for the large tip gap than for the small tip gap. It is also apparent that near the leading edge of the blade there is a longer path length across the tip for the streamlines with the large tip gap. For the large tip gap the streamlines exit the gap further downstream along the suction surface resulting in a larger velocity differential between the local passage flow and the tip gap flow. It is this velocity differential combined with a larger leakage flow that leads to a larger vortex formation for the large gap.

The tip leakage vortex is shown in Figures 6a-b for the two gap sizes. These secondary flow vectors are shown for a flow plane that is near the exit of the blade passage (92% of the axial chord) where the plane has been taken normal to the suction surface of the blade. The transformed v- and w-components (V_n and V_z) are plotted as a function of the distance perpendicular to the blade (Y) and distance down from the shroud (-Z). Figures 6a-b indicate the size of the tip leakage vortex for the two gap sizes, which dominates most of the passage for the large tip gap. The CFD predictions indicate that the leakage vortex is shifted slightly closer to the blade surface for the small tip gap. The vortex centers are located at Y/P = 0.10 and Z/S = -0.05 for the small tip gap and Y/P = 0.20 and Z/S = -0.07 for the large tip gap. The outward flow near Y/P = 0.3 is a result of the fluid being entrained into the wake region of the adjacent blade. Although not shown here, the vortex size and location appears to be only a function of tip gap size and did not significantly vary with the blowing ratios explored in this investigation.

Effect of Tip Geometry

Effects of the tip geometry were made by comparing a flat tip to a tip with a dirt purge cavity with no flow exiting the dirt purge holes. As discussed previously, Figure 5a and 5b show streamlines released from an upstream plane that is at 1.5 tip gap heights below the shroud for a flat tip with large and small tip gaps, respectively. Figures 5c and 5d show streamlines released from the same location relative to the shroud for blade tips that have a dirt purge cavity with no blowing from the dirt purge. For the tip having the purge cavity, it is clear that the tip flow streamlines are drawn into the front end of the dirt purge cavity prior to exiting out of the trailing edge of the cavity. As the streamlines approach the back of the cavity, the flow stagnates on the downstream cavity wall. A strong positive spanwise velocity component is present as the flow exits the cavity and is directed away from the tip. There is no effect of the non-flowing cavity on the downstream tip leakage vortex nor are there any significant changes over the latter half of the blade.

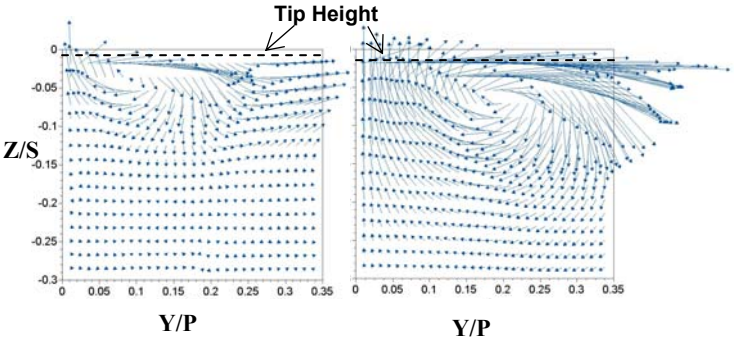

Figures 6a-b. Secondary flow vectors along a suction side plane at an axial chord location of 92% for a flat tip with no blowing and a) a small tip gap, and b) a large tip gap. Location of the plane is shown in Figure 5a and b.

Effect of Dirt Purge Blowing

As was indicated in Table 2, computations were performed at each tip gap with two coolant flows through the dirt purge (0.19% and 0.29% passage flow). For these computations, the energy equation was also solved such that the cooling effectiveness from the dirt purge holes could be assessed. Adiabatic boundary conditions were applied to all surfaces. Static pressure contours are shown in Figures 7a and 7b for the high blowing cases with the small and large tip gaps. It is clear from the static pressure distributions that the dirt purge blowing has a large effect locally on the static pressure distribution along the blade tip and shroud as compared with the flat blade tip (Figures 3a and 3c). This effect can be particularly seen in the region of the dirt purge cavity. There is a large region in the leading edge of the blade and shroud indicating the same static pressure as that of the inlet. The leading edge region is shown to have the same static pressure as the inlet as a result of the dirt purge blowing, which acts as a flow blockage to the tip leakage. These blockage effects will be discussed further in the next section. There are very high static pressures above the dirt purge holes as the jets impinge upon the shroud. The largest difference that can be seen between Figures 7a and 7b are shown on the shroud with lower static pressures for the larger tip gap, which indicate higher leakage flows. In addition, there is a low static pressure contour indicated on the shroud for the large tip gap resulting from the tip vortex formation.

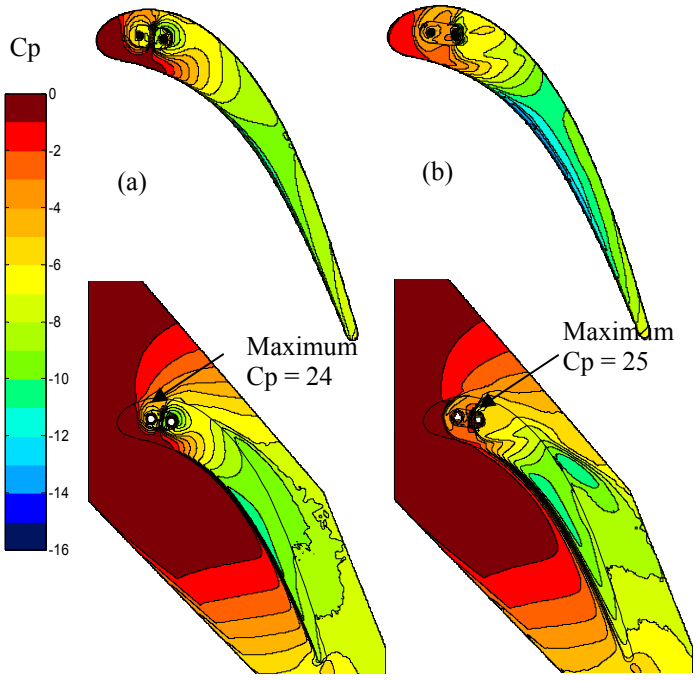

Figures 7a-b. Pressure coefficient predictions on the tip and shroud for the high blowing case (0.29%) for the a) small tip gap and b) large tip gap.

Figures 8a-b show streamlines that have been released from 1.5 gap heights down from the shroud for the small and large tip gap cases with 0.29% coolant injection from the dirt purge. Figures 8c-d, cut through the dirt purge cavity and show the velocity vectors superimposed onto the thermal field for the same cases. The white lines in Figures 8a-b show the location for Figures 8c-d. Relevant comparisons for these streamlines can be made to those shown in Figures 5a-d. In comparing these figures, there is a large effect in the streamline pattern with the presence of injected coolant from the dirt purge as compared with the no injection cases. Clearly, one can observe the absence of streamlines over the leading edge portion of the blade near the cavity for the small tip gap (Figure 8a). These predictions indicate that the dirt purge injection acts as a blockage for the tip leakage flow. While it is clear that a tip leakage vortex does form for the case with blowing purge holes, the initial formation of this vortex occurs further downstream along the suction surface than for the case with no blowing. The predictions for the larger tip gap, shown in Figure 8b, indicate that even for the high blowing conditions the dirt purge injection did not effectively block the leakage flow. The streamlines for the large tip gap do indicate that the leakage flow wraps around the purge jets in a horseshoe.

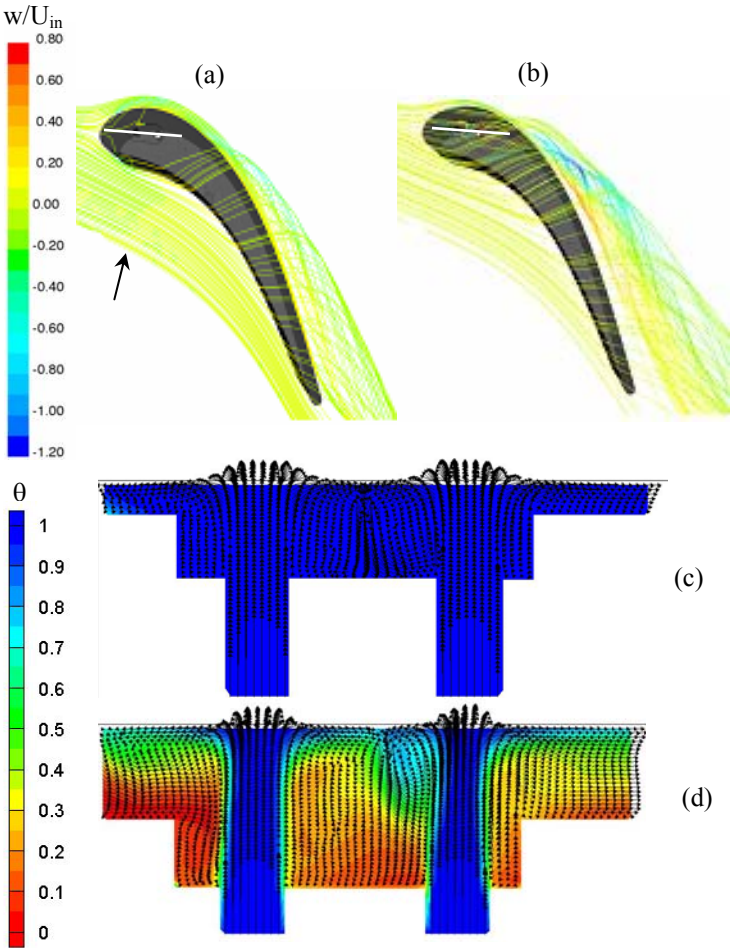

Figures 8a-d. Streamline predictions with 0.29% dirt purge blowing at the small tip gap (a and c) and the large tip gap (b and d). Streamlines released from 1.5 tip gap heights below the shroud and are colored by spanwise velocity. Velocity vectors and thermal field contours are shown in the tip gaps for the (c) small and (d) large tip gaps.

The flow and thermal fields within the dirt purge cavity, shown in Figure 8c for the small tip gap, indicate cool fluid throughout the region. The flow field predictions indicate four asymmetric vortical patterns within the purge cavity. Figure 8d indicates a much different thermal field and vortical pattern for the larger tip gap. As the jet impinges on the shroud there is a relatively weak and strong vortex set up on the windward and leeward sides of the cavity, respectively. The coolant from the dirt purge is not sufficient to block the leakage flows and as a result there is a large amount of stagnant hot gas within the dirt purge cavity.

Adiabatic effectiveness levels on the blade tip and shroud were computed for the four cases described above (two tip gaps with each at two blowing ratios). These effectiveness levels are based on the computed adiabatic wall temperature, inlet temperature of the primary gas, and coolant temperature through the dirt purge holes.

Figures 9a-b depict the predicted effectiveness results on both the tip and shroud obtained for the small tip gap while Figures 10a-b depict the effectiveness for the large tip gap case. The two coolant flows that were considered for both cases are 0.19% and 0.29% coolant flow relative to the core flow. Table 3 lists the relation between the coolant flow addition and the

Table 3. Mass/Momentum Flux Ratios for the Coolant Flow.

% Coolant Mass Flow	Mass flux Ratio	Momentum flux Ratio
0.05	0.9	0.6
0.1	1.8	2.6
0.19	3.7	8.7
0.29	5.5	20.7
0.38	7.4	34.8

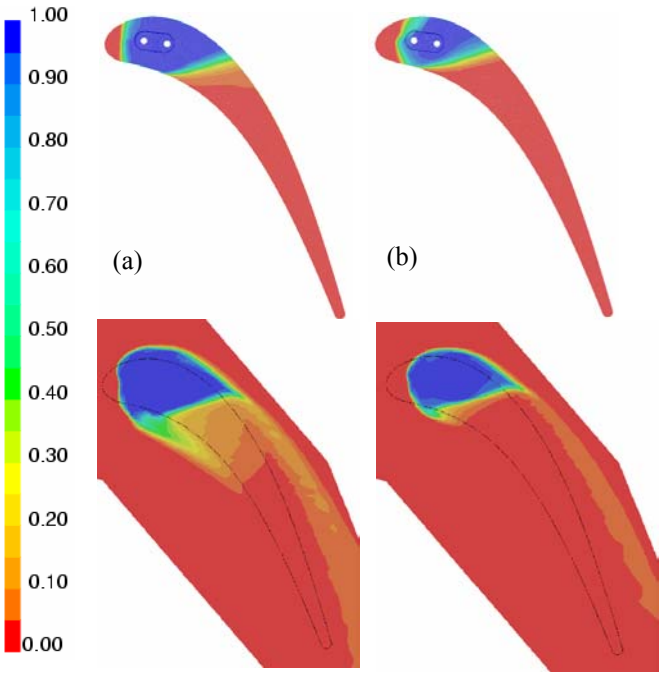

Figures 9a-b. Predictions of adiabatic effectiveness for tip and shroud for the small tip gap for two different blowing conditions at a) 0.29% and b) 0.19% of the core flow.

mass and momentum flux ratios. Note that these ratios are based on the total upstream incident velocity (U_{in}) and density (used in the denominator of the ratios), rather than the local crossflow velocity. There is only a slight difference in the predicted effectiveness levels between the two coolant flow conditions for the small tip gap, as shown in Figure 9a-b. For both cases, the coolant from the dirt purge holes only covers the first one-third of the blade. It is somewhat unexpected that coolant is transported such that there is a cool region extending across the entire pitch of the blade tip from the pressure to suction sides. The leading edge region of the tip, however, remains uncooled for the small tip gap. The shroud shows similar cooling levels over the dirt purge cavity. Some of the coolant continues to scour the shroud in the passage region as a result of the coolant being transported by the tip leakage vortex.

As the gap size increases with blowing ratios of 0.19% and 0.29%, shown in Figure 10a-b, there is a drastic reduction in the predicted effectiveness levels for the blade tip and, to a lesser extent, for the shroud. The increase in tip gap allows for significantly more leakage flow. It is expected that dirt purge coolant would be seen directly downstream of the purge holes, but for a large tip gap with 0.29% blowing there is little cooling in the vicinity of the dirt purge. In fact, at the large tip gap the exhausted coolant flow appears to only impinge the shroud and then slightly sweep the blade tip. This motion creates swirling vortices over the top of the blade around the dirt purge. These vortices, to be discussed in the next section, explain the unusual cooling patterns displayed for a large gap at 0.29% blowing.

Figures 11a-b present the pitchwise-averaged adiabatic effectiveness over the blade tip and shroud, respectively. As seen with the contour plots and confirmed with these averaged effectiveness plots, the best effectiveness results occur for a case when the tip gap is small and the blowing ratio is at 0.29%. At small tip gaps, the averaged blade effectiveness reaches values very close to one with the cooling generally seen over the entire leading edge of the blade. For the small gap, the averaged effectiveness levels do not show a substantial decrease as the coolant is decreased from 0.29% to 0.19%. There is, however, a significant reduction in the averaged effectiveness levels for the large gap as compared with the small gap indicating that the cooling is largely influenced by the tip gap size. The large gap results show that the maximum averaged effectiveness levels on the blade tip are near $\overline{\eta} = 0.15$ for both high and low flow conditions. None of the four cases provided any cooling for the leading edge of the blade tip.

Some of the same general cooling trends seen on the tip are consistent with the shroud as can be seen in Figure 11b. The averaged effectiveness levels are lower, in general, for the shroud as compared with the tip because of the larger surface area for the shroud. The averages were computed across the entire pitch of the shroud for a given axial location. These averaged effectiveness levels follow the same trends and are generally offset from each other proportional to the blowing ratio. The blowing does not reach the leading edge of the blade, but it does affect the shroud slightly further upstream than was seen on the blade tip. This is due to the physical extent of the shroud surface which is approximately 20 times the size of the tip. Figure 11b illustrates that there is significant cooling on the shroud, which is higher than on the blade tip for the larger tip gap size.

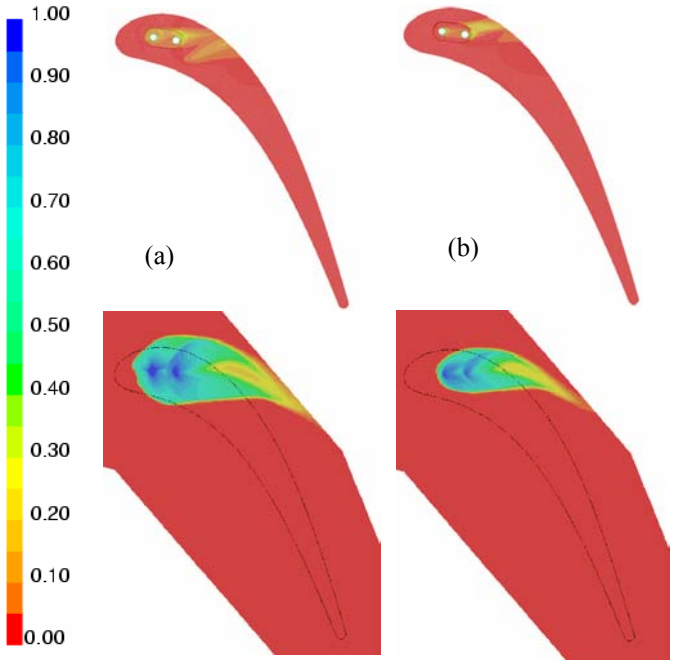

Figures 10a-b. Predictions of adiabatic effectiveness for the tip and shroud for the large tip gap for two different blowing conditions at a) 0.29% and b) 0.19% of the core flow.

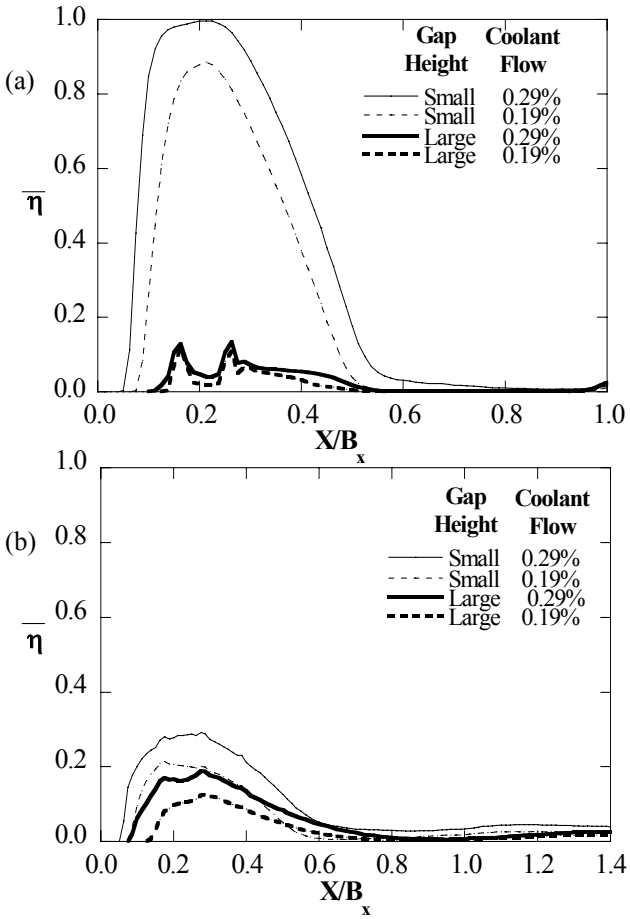

Figures 11a-b. Comparison of pitchwise-averaged effectiveness on the a) blade tip and b) shroud.

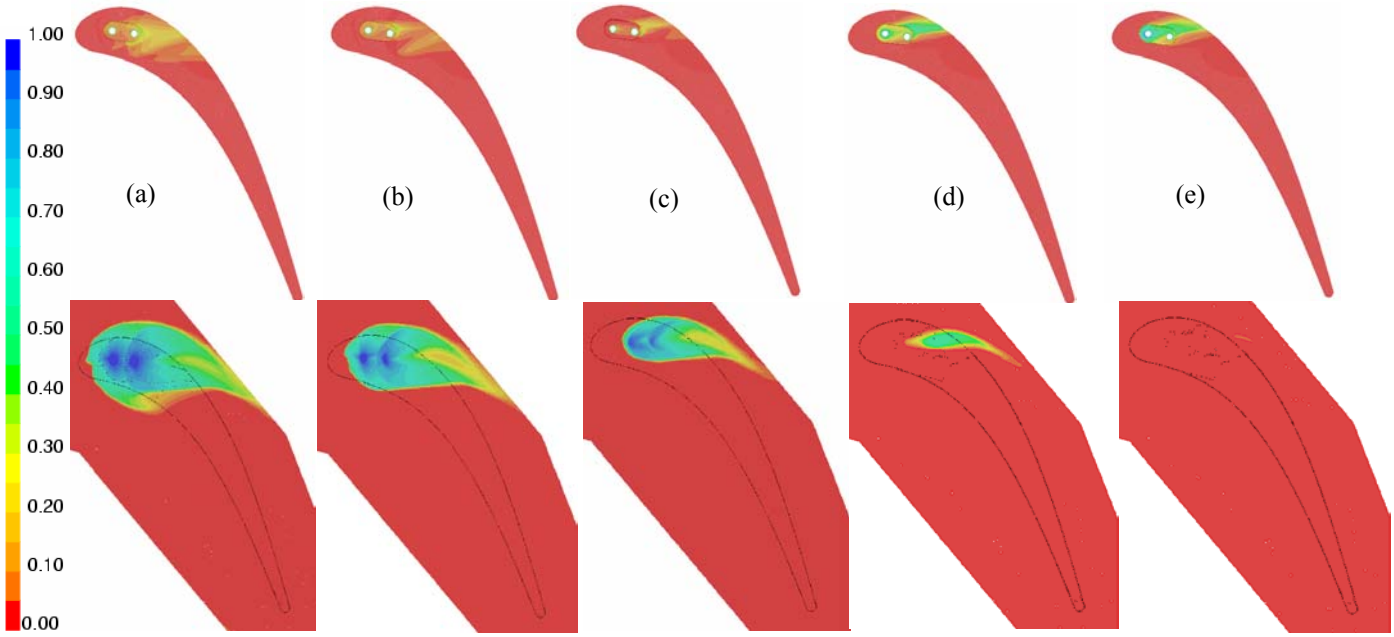

Figures 12a-e Contour plots of adiabatic effectiveness on the blade tip and shroud for a large tip gap with coolant released at values of a) 0.38%, b) 0.29%, c) 0.19%, d) 0.10% and e) 0.05%.

EFFECT OF BLOWING FOR A LARGE TIP GAP

As discussed, the initial computational work focused on testing two blowing ratios (0.19% flow and 0.29% flow) and two tip gap heights (0.54% span and 1.63% span). This produced relatively good cooling in the leading edge region for the small tip gap, but relatively poor cooling for the large tip gap. This poor effectiveness at large tip gaps results from the increased leakage flow coupled with the relatively high momentum jets exhausting from the dirt purge that primarily impact the shroud. The coolant flow exhausts from the dirt purge holes in the blade, impacts the shroud, and is then transported away by the leakage flow. At the smaller tip gap the leakage flow is significantly lower and there is less distance between tip and shroud allowing for coolant flow to impact both the blade tip and shroud before exiting the tip gap.

To determine which coolant flows would become effective for the tip of the blade and to gain a better understanding of the dirt purge cooling, a range of blowing ratios were examined. The range of coolant flows went from 0.05% to 0.38% of the total passage exit flow. Note that the corresponding mass flux ratios and momentum flux ratios for these cases are listed in Table 3. The effectiveness predictions for the different cases are shown in Figures 12a-e for the large tip gap.

At the highest blowing ratio, the effectiveness levels on the tip indicate the largest coverage although the effectiveness levels are relatively low ($\eta \sim 0.25$). Similar to that discussed previously, the effectiveness pattern that is occurring results from the jet impingement on the shroud after which the jet is re-directed onto the blade tip. The shroud, on the other hand, is cooled fairly well with only a small region near the leading edge of the tip that is uncooled. As the blowing ratio is decreased, the cooling on the tip decreases until the 0.19% coolant flow condition. In reducing the coolant flow below 0.19%, the effectiveness levels remain at approximately $\eta = 0.25$, but this cooling is only found in a narrow region of the blade. At the lower blowing ratios, the increased tip cooling was due to the lower momentum jets from the dirt purge ducts. Instead of impacting the shroud, the flow remains somewhat attached to the tip resulting in increased blade tip cooling. As the coolant flow from the dirt purge jets is reduced the effectiveness on the shroud continually decreases until it is essentially non-effective for the 0.05% cooling flow case as indicated in Figures 12a-e.

Streamlines injected from the dirt purge holes are shown in Figures 13a-b for the 0.10% and 0.29% coolant flow cases. For the 0.10% coolant flow condition, the streamlines hug the blade tip as the leakage flow deflects the jet penetration. For the 0.29% coolant flow case, it is clear that the jets impinge upon the shroud and then form vortices as the coolant flow interacts with the gas path leakage flow. These vortices convect some of the dilute jet coolant onto the blade tip at the higher coolant flow case.

Figures 14a-b depict the pitchwise-averaged adiabatic effectiveness over the blade tip and shroud, respectively. Note that the sides of the cavity were not used in these pitchwise averages, but the bottom of the cavity was used. All five cases show the coolant flow affecting the blade at approximately 10% axial chord. These pitchwise-averaged effectiveness values indicate the maximum levels for the 0.05% coolant flow condition closest to the blade leading edge. These pitchwise-averages continue to decrease with increasing coolant injection until the 0.19% coolant flow condition. Increasing the coolant above 0.19% coincides with increased effectiveness levels. The two peaks in the effectiveness curves are a result of the jet being redirected onto the blade tip.

Pitchwise-averaged adiabatic effectiveness levels are depicted in Figure 14b for the shroud. Levels of effectiveness reach as high as 0.25 and decrease to a level of zero as the coolant injection is decreased from 0.38% to 0.05%. For 0.38%, 0.29% and 0.19% flow the curves are proportional to the amount of coolant from the dirt purge jets. With 0.10% flow there is a small shift in the peak cooling while for the lowest blowing ratio, the coolant does not impact the shroud.

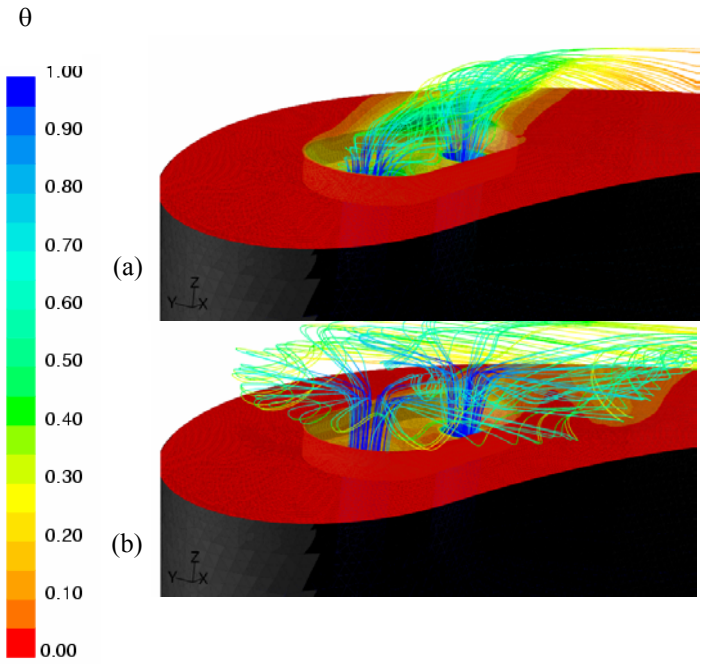

Figures 13 a-b. Streamlines released from the dirt purge holes for the small tip gap at a) 0.10% and b) 0.29% coolant flowrates.

To obtain effectiveness for each of the respective flow geometries and blowing ratios tested, an area-weighted average adiabatic effectiveness was calculated over the tip and shroud. Figure 15 shows the effectiveness as a function of percentage of cooling flow from the dirt purge holes. It is clearly evident that for a value of 0.19% coolant, a minimum effectiveness level occurs on the tip. It is also clear that even by increasing the blowing for the large tip gap to twice that considered for the small tip gap, the results indicate that the same high effectiveness levels could not be achieved for the large tip gap as compared with the small tip gap.

Cooling on the shroud for a large tip gap does not follow the same trend that was seen on the blade tip. Instead, the curve shows a nearly linear increase in cooling as more coolant is released from the dirt purge. The cooling differences between the small and large tip gaps are not as large for the shroud as compared with the tip.

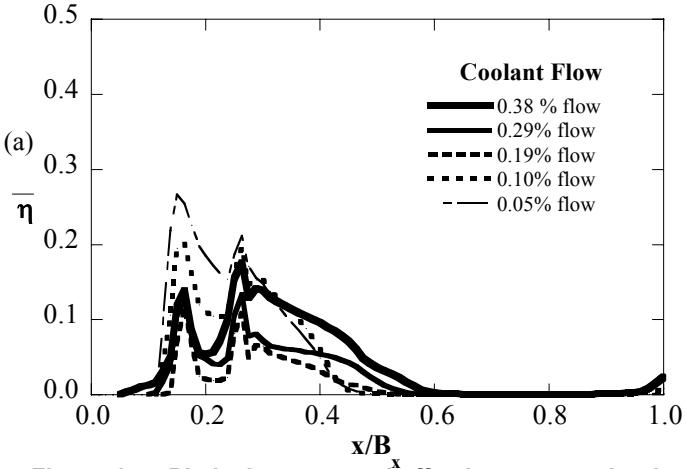

Figure 14a. Pitchwise-averaged effectiveness on the tip for the large tip gap cases.

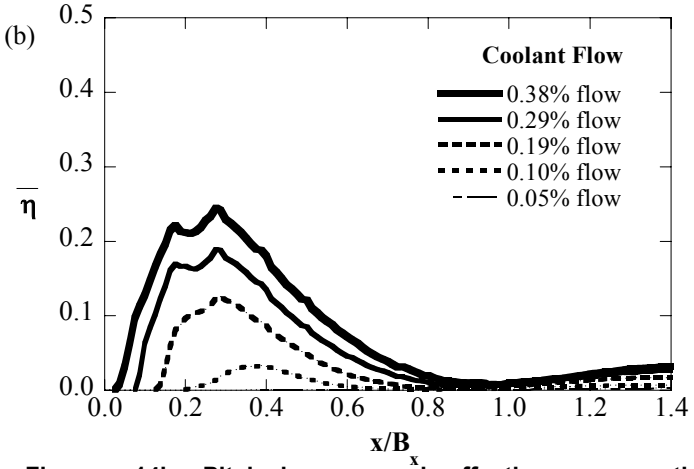

Figures 14b. Pitchwise-averaged effectiveness on the shroud for the large tip gap cases.

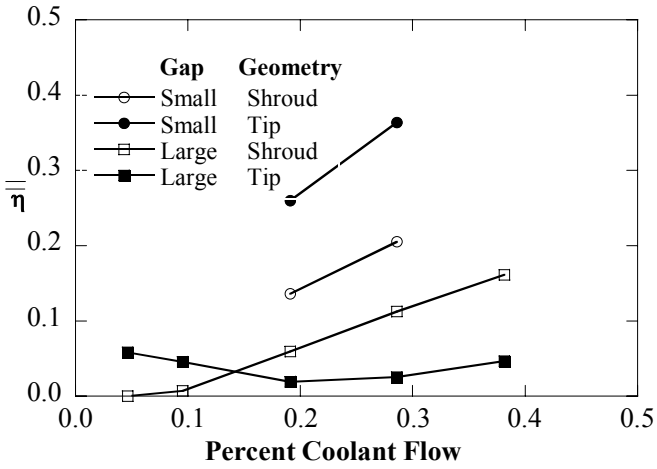

Figure 15. Area-averaged adiabatic effectiveness on the blade tip and shroud as a function of blowing ratio.

CONCLUSIONS

A number of simulations have been performed for this study that have addressed various effects on the blade tip leakage flows and cooling strategies. The size of the tip gap has a large impact on the amount of leakage flow as well as on the formation of the tip leakage vortex. Having a non-flowing purge cavity in the blade tip did not have an overall effect on the tip leakage flows nor on the tip leakage vortex.

Cooling on the blade tip and shroud were computed for a case where coolant was injected through dirt purge holes. These purge holes are necessary in most turbine designs for extracting dirt that is ingested by the compressor. The flow injected from the blade tip through these dirt purge holes serve to block the leakage through the tip gap. This blockage worked quite well for the small tip gap that was studied, but was not as effective for the large tip gap.

To further improve the cooling on the blade tip and shroud for the large tip gap, a of number computations were completed that simulated a range of blowing ratios for the dirt purge. These results indicated that as the blowing ratios increased, the effectiveness levels on the shroud also increased; however, the effectiveness levels on the tip actually decreased until a

minimum was reached. As the blowing ratios were further increased, the effectiveness levels also started to increase for the blade tip. This minimum effectiveness for the blade tip occurred as a result of large amounts of hot gas leakage through the tip gap combined with a low coolant flow injection into the tip gap whereby most of the coolant did not come into contact with the blade tip. These results indicated that for a large tip gap, there are definite cooling strategies that are more effective than others.

NOMENCLATURE

B_x = axial chord
C = true chord of blade
C_p = pressure coefficient, $C_p=(p - p_{in}) / (\rho U_{in}^2 / 2)$
I = momentum flux ratio, $I = \rho_c U_c^2 / \rho_{in} U_{in}^2$
$\dot{m}$ = mass flowrate
M = mass flux ratio, $M = \rho_c U_c / \rho_{in} U_{in}$
P = blade pitch
P_o, p = total and static pressures
Re_{in} = Reynolds number defined as $Re_{in} = C\ U_{in} / \nu$
s = surface distance along blade from stagnation
S = span of blade
T = temperature
U,V,W = global, mean streamwise velocity component
X,Y,Z = global coordinates defined by blade stagnation
u,v,w = in-plane velocity components
V_s = transformed streamwise velocity, $u\cos\psi_{ms} + v\sin\psi_{ms}$
V_n = transformed normal velocity, $-u\sin\psi_{ms} + v\cos\psi_{ms}$
V_z = spanwise velocity, w

Greek

η = adiabatic effectiveness, $\eta = (T_{in} - T_{aw})/(T_{in} - T_c)$
θ = normalized thermal field, $\theta = (T_{in} - T)/(T_{in} - T_c)$
Δ = denotes a difference in value
ψ_{ms} = midspan turning angle, $\tan^{-1}(v_{ms}/ u_{ms})$
ρ = density
ν = kinematic viscosity

Subscripts

ave, $\overline{}$ = pitchwise average at a given axial location
ave, $\overline{\overline{}}$ = area average
aw = adiabatic wall
c = coolant conditions
in = value at 1C upstream of blade
ms = value at blade midspan
max = maximum value

ACKNOWLEDGMENTS

The authors would like to acknowledge support from Pratt and Whitney for the work presented in this paper. In particular, Mike Blair, Frank Cunha, Tom Praisner, and John Wiedemer are to be thanked for their contributions to this work.

REFERENCES

[1] Bunker, R. S. "A Review of Turbine Blade Tip Heat Transfer," Turbine 2000 Symposium on Heat Transfer in Gas Turbine Systems, Cesme, Turkey, 2000.

[2] Bunker, R. S. "Heat Transfer and Flow on the First-Stage Blade Tip of a Power Generation Gas Turbine: Part 1-Experimental Results," *J of Turbomachinery*, **122**, pg. 263-271, 2000.

[3] Papa, M., Goldstein, R. J., Gori, F., "Effects of Tip Geometry and Tip Clearance on the Mass/Heat Transfer from a Large-Scale Gas Turbine Blade," GT-2002-30192.

[4] Azad, G., Han, J.C., and Teng, S., "Heat Transfer and Pressure Distributions on a Gas Turbine Blade Tip," 2000-GT-194.

[5] Acharya, S., Yang, H., Ekkad, S.V., Prakash, C., Bunker, R., "Numerical Simulation of Film Cooling Holes On the Tip of a Gas Turbine Blade," GT-2002-30553.

[6] Kim, Y. W., Downs, J. P., Soechting, F. O., Abdel-Messeh, W., Steuber, G., and Tanrikut, S., "A Summary of the Cooled Turbine Blade Tip Heat Transfer and Film Effectiveness Investigations Performed by Dr. D. E. Metzger," *J of Turbomachinery*, **117**, pp. 1-11, 1995.

[7] Kwak, J. S. and Han, J. C., "Heat Transfer Coefficient and Film-Cooling Effectiveness on a Gas Turbine Blade Tip," GT-2002-30194.

[8] Metzger, D. E., Bunker, R. S., Chyu, M. K., "Cavity Heat Transfer on a Transverse Grooved Wall in a Narrow Flow Channel," *J of Heat Transfer*, **111**, pp. 73-39, 1989.

[9] Chyu, M. K., Moon, H. H., and Metzger, D. E., "Heat Transfer in the Tip Region of Grooved Turbine Blades," *J of Turbomachinery*, **111**, pp. 131-138, 1989.

[10] Fluent Inc., Fluent User's Guide, Version 6.0, 2002 (Fluent Inc.: New Hampshire).